

# r-Process Nucleosynthesis in Neutrino-Driven Winds from a Typical Neutron Star with $M = 1.4M_{\odot}$

M. Terasawa<sup>1</sup>, K. Sumiyoshi<sup>2</sup>, S. Yamada<sup>3</sup>, H. Suzuki<sup>4</sup>, and T. Kajino<sup>1</sup>

## ABSTRACT

We study the effects of the outer boundary conditions in neutrino-driven winds on the r-process nucleosynthesis. We perform numerical simulations of hydrodynamics of neutrino-driven winds and nuclear reaction network calculations of the r-process. As an outer boundary condition of hydrodynamic calculations, we set a pressure upon the outermost layer of the wind, which is approaching toward the shock wall. Varying the boundary pressure, we obtain various asymptotic thermal temperature of expanding material in the neutrino-driven winds for resulting nucleosynthesis. We find that the asymptotic temperature slightly lower than those used in the previous studies of the neutrino-driven winds can lead to a successful r-process abundance pattern, which is in a reasonable agreement with the solar system r-process abundance pattern even for the typical proto-neutron star mass  $M_{NS} \sim 1.4M_{\odot}$ . A slightly lower asymptotic temperature reduces the charged particle reaction rates and the resulting amount of seed elements and lead to a high neutron-to-seed ratio for successful r-process. This is a new idea which is different from the previous models of neutrino-driven winds from very massive ( $M_{NS} \sim 2.0 M_{\odot}$ ) and compact ( $R_{NS} \sim 10$  km) neutron star to get a short expansion time and a high entropy for a successful r-process abundance pattern. Although such a large mass is sometimes criticized from observational facts on a neutron star mass, we dissolve this criticism by reconsidering the boundary condition of the wind. We also explore the relation between the boundary condition and neutron star mass, which is related to the progenitor mass, for successful r-process.

*Subject headings:* r-process nucleosynthesis, supernova, neutron star

---

<sup>1</sup>National Astronomical Observatory, Osawa, Mitaka, Tokyo 181-8588, Japan

<sup>2</sup>Numazu College of Technology, Ooka, Numazu, Shizuoka 410-8501, Japan

<sup>3</sup>Institute of Laser Engineering (ILE), Osaka University, Yamadaoka, Suita, Osaka 565-0871, Japan

<sup>4</sup>Faculty of Science and Technology, Tokyo University of Science, Yamazaki, Noda, Chiba 278-8510, Japan

## 1. Introduction

The r-process nucleosynthesis, which is a rapid neutron capture process faster than beta-decay, is believed to be responsible for about a half of elements heavier than iron (Burbidge et al. 1957). Many heavy elements presumably produced in the r-process have recently been detected in extremely metal-poor stars by recent astronomical observations (Snedden et al. 1996, 1998, 2000, Westin et al. 2000, Johnson and Bolte 2001, Cayrel et al. 2001, Honda 2001). Their abundance pattern proves to be very similar to the one of the solar r-process pattern, which is called the universality in the r-process abundance pattern, especially in the region of  $56 \leq Z \leq 70$ . This universality of abundance pattern strongly suggests that the r-process occurs in the same way independently of the metallicity along the entire history of Galactic chemical evolution from the beginning of the Galaxy to the present. It means simultaneously the fact that the origin of the r-process is most likely in supernovae (SNe) of massive progenitor stars since massive stars first evolve and end up with SN explosions whose ejecta reflects abundances in metal-poor stars.

One of the most plausible sites of the r-process is the neutrino-driven winds in supernovae. Woosley et al. (1994) have demonstrated that the very high entropy conditions,  $\sim 400 k_B$ , are realized in the neutrino-driven wind and on these specific conditions the r-process nucleosynthesis occurs successfully. This r-process scenario in high entropy hot bubble has been later pointed out to be rather difficult because copious supernova neutrinos change neutrons to protons and hinder the r-process (Meyer 1995). In more recent studies, the successful r-process pattern in the neutrino-driven winds has been obtained even for relatively low entropy,  $\sim 200k_B$ , provided that the expansion time scale is much shorter,  $\sim 10$  ms, than the time scale of the neutrino process (Otsuki et al. 2000, Sumiyoshi et al. 2000), making the neutrino-driven wind scenario viable again. However, they assumed a large neutron star mass,  $\sim 2.0M_\odot$ , in order to gain a slightly higher entropy. These parameter setups have been referred with caution because the observed neutron star has a typical mass  $\sim 1.4M_\odot$  and a radius  $\sim 10$  km.

In this paper we will discuss that the outer boundary conditions of the neutrino-driven winds may resolve this problem of the neutron star mass. It has recently been founded (Terasawa et al. 2001) that the r-process occurs far from the neutron star in a less dense region rather close to and behind the outward shockwave after the surface material is blown off. It is generally known that alpha captures are very sensitive to the temperature. A little change in temperature can make a large effect on the abundance of seed elements and heavy r-process elements. This effect on nucleosynthesis of outer region has not been studied very well. In most previous studies, the boundary condition of outer region has been chosen based on the results by Woosley et al. (1994). This is because their simulation is the unique

simulation which deals with both supernova explosion and neutrino-driven wind at once. In their study the temperature is about 0.1 MeV and the density is  $\sim 10^3$  g/cm<sup>3</sup> at the outer boundary (at radius of  $10^4$  km).

The physical condition in the outer boundary region depends on the competition between the falling matter from the envelope and the outward shockwave, giving many factors to change by a core bounce. There are a lot of factors to effect the boundary condition. We perform the hydrodynamical simulations of neutrino-driven winds and investigate the dependence of the r-process nucleosynthesis on the pressure of the outer material, toward which the wind blows, behind the shockwave. We show that the successful r-process can occur in the neutrino-driven winds from a typical neutron star mass with  $1.4M_{\odot}$  by choosing a slightly lower pressure and temperature than those adopted previously. We also examine the dependence of the r-process yields on the neutron star mass in order to assess the relation between the stellar mass and the outer boundary condition. Since a different mass of progenitor star is suggested to lead to a different mass of envelope and remnant mass, we infer a correspondence between the progenitor mass and the outer boundary condition to realize the universality and successful the r-process abundance pattern. This study is important to constrain the mass range of progenitor stars that culminate their evolution for collapse-driven supernovae as the source of the r-process elements which are observed in very metal-poor stars.

## 2. Models of Proto-Neutron Star and Neutrino-Driven Winds

In collapse-driven supernovae, the shockwave launches at the bounce of central part of collapsing iron core and a proto-neutron star forms after the core bounce. A hot and less-dense region, which is often called a hot bubble, above the proto-neutron star behind the shockwave is believed to be an ideal site for the r-process. Thin surface layer of the proto-neutron star is heated by intense flux of neutrinos, increasing the entropy and forming a neutrino-driven wind as a hot and less-dense gas. Thus, the wind is finally blown off toward the shockwave from behind. At this time the shockwave has already been propagating outward further at  $\sim 10^3 - 10^4$  km.

We perform numerical simulations of the hydrodynamics of the thin layer of the proto-neutron star, which is parameterized by mass and radius, to obtain the temporal information of thermodynamical conditions for nucleosynthesis. The details of the numerical simulation can be found in Sumiyoshi et al. (2001). We employ the implicit lagrangian code for general relativistic and spherically symmetric hydrodynamics (Yamada 1997) including the heating and cooling processes due to neutrinos (Qian and Woosley 1996). The average energy of

neutrinos is set equal to 10 MeV for electron-type neutrinos, 20 MeV for electron-type anti-neutrinos, and 30 MeV for  $\mu$ - and  $\tau$ -neutrinos and their anti-neutrinos, as adopted in the previous studies (Qian and Woosley 1996, Otsuki et al. 2000, Sumiyoshi et al. 2000). We set the neutrino luminosity  $L_{\nu_i} = 1 \times 10^{51}$  erg/s for each species ( $i = e, \nu, \tau$ ) and it is set to be constant during the simulation. Accordingly, the total luminosity is  $L_{\nu}^{total} = 6 \times 10^{51}$  erg/s. The neutrino distribution function is set at each lagrangian grid point instead of solving the Boltzmann equation (Yamada, Janka & Suzuki 1999). We use the extended table of the relativistic equation of state (Shen et al. 1998a, 1998b, Sumiyoshi et al. 2001).

We adopt a neutron star with the typical mass,  $M_{NS} = 1.4M_{\odot}$ , and the radius,  $R_{NS} = 10$  km, as an inner boundary condition. We obtain the initial structure of thin layer above this neutron star by solving the Oppenheimer-Volkoff equation of the hydrostatic equilibrium. The density range of this layer is from  $10^{11}$  to  $5 \times 10^6$  g/cm<sup>3</sup> and the covered baryon mass is about  $10^{-5}M_{\odot}$ . This means that surface material is thin enough and the assumption of constant temperature and constant electron fraction holds well. For simplicity, we set the temperature to 3 MeV and the electron fraction to 0.25 in the whole material as typical values. The results are not sensitive to these values.

As an outer boundary condition, we put a constant pressure next to the outermost grid point of lagrangian mesh. We parameterize this pressure of a uniform gas as the outer boundary pressure,  $P_{out}$  and study its effect on the neutrino-driven wind and a subsequent r-process. This pressure does not influence the wind near the surface of a neutron star, because  $P_{out}$  is much smaller than the pressure of the whole layer at high density. It acts as a deceleration of the expansion only when the pressure of the material becomes close to the  $P_{out}$  value. The pressure approaches this value asymptotically as the wind material goes far away from a neutron star. Accordingly, the temperature of wind material also approaches a final temperature  $T_{out}$ , corresponding to  $P_{out}$ , since the pressure is dominated by radiation. A choice of the outer boundary pressure has apparently a big influence on the r-process nucleosynthesis because the r-process takes place most efficiently when the wind material arrives at the region just behind the shockwave (Terasawa et al. 2001). This fact demands fairly careful studies of the outer boundary conditions in supernova explosions.

In most previous studies of neutrino-driven winds, the boundary condition of temperature has been uniquely chosen to 0.1 MeV at radius  $10^4$  km according to the pioneering study of Woosley et al. (1994). The value of outer boundary pressure,  $P_{out}$ , was taken to be  $10^{22}$  dyn/cm<sup>2</sup> in the previous hydrodynamical study of the neutrino-driven wind (Sumiyoshi et al. 2001) to match with the temperature of about 0.1 MeV. The  $P_{out}$  value, however, should change in a certain allowed range because the thermodynamical conditions of the region between the neutron star surface and the shockwave may depend on each progenitor star.

This means that a higher  $P_{out}$  value might correspond to a more massive star associated with more massive envelope and a larger iron core, which may be related with both neutron star mass and outer boundary pressure. In principle it should be determined by the configuration of progenitor and the passage of the shockwave. It is, therefore, necessary to carry out the numerical simulations of the whole dynamic processes from core-collapse to explosion in order to determine the conditions precisely. Analytical studies of shock propagation are also important in order to evaluate the pressure value behind the shock wall.

In the current study we vary the outer boundary pressure as  $P_{out} = 10^{20}, 10^{21}, 10^{22}$  dyn/cm<sup>2</sup> so as to cover reasonable range for various supernova environments instead of carrying out numerical simulations of the whole dynamics. These pressure correspond to final temperatures ranging  $T_9 \sim 0.4 - 1.3$ . Note that a higher pressure such as  $10^{23}$  dyn/cm<sup>2</sup> is not used since only the iron group elements are finally synthesized by dominating alpha-capture reactions due to the high temperature  $0.1 \text{ MeV} < T_{out}$ , which is irrelevant in the present studies of the r-process nucleosynthesis.

We perform a set of numerical simulations for different  $P_{out}$  values and take out one of trajectories from the lagrangian mesh in each simulation for nucleosynthesis calculations. We summarize in Table 1 the key quantities for the r-process nucleosynthesis from the numerical results of hydrodynamical simulations. In this table  $\tau_{dyn}$ ,  $S$ ,  $Y_{e,i}$  and  $T_{out}$  stand for the dynamical timescale, the entropy per baryon (in the unit of the Boltzmann constant), the initial electron fraction for nucleosynthesis when the temperature drops to  $T_9 = 9.0$ , and the asymptotic temperature (in the unit of  $10^9$  K) of the expanding wind material. We call this asymptotic temperature as the outer boundary temperature since the temperature approaches this value to be determined by the outer boundary pressure. Note that the definition of  $\tau_{dyn}$  is the  $e$ -fold time at  $T = 0.5$  MeV, which is conventionally used to characterize the duration of the alpha-process. Let us emphasize that the expansion timescales in our model calculations are a few times larger than those in the previous models,  $\tau_{dyn} \leq 10$  ms, which lead to a successful r-process abundance pattern (Otsuki et al. 2001, Sumiyoshi et al. 2001). Nevertheless, the expansions in all calculated models are rapid enough so that the r-process occurs promptly even at asymptotic region close to the shock wall without hindrance by the neutrino-process (Meyer 1995).

We show the time evolution of the temperature,  $T_9$ , in the upper panel of Fig. 1. The dashed, solid, dotted lines are the results in the cases of  $P_{out} = 10^{20}, 10^{21}, 10^{22}$  dyn/cm<sup>2</sup>, respectively. Note that the dynamics of the winds is similar to one another among three cases at the temperature  $T_9 \geq 7$ , below which a gradual departure towards the final stage of different outer boundary conditions of  $P_{out}$  and  $T_{out}$  can be seen. The time evolutions of the abundances of alpha particles and seed nuclei are different among three cases, as

shown in Fig. 1, due to the different temperature variation below  $T_9 = 7$ . These differences lead to a significant difference in the products of the r-process nucleosynthesis. In Table 1,  $Y_{\alpha,out}$  and  $Y_{seed,out}$  are the final abundances of alpha particles and the sum of seed nuclei ( $70 \leq A \leq 120$ ) at the final stage of our nucleosynthesis calculations. The details of these quantities are discussed in the next section.

### 3. Results of the Nucleosynthesis calculations

We employ the reaction network including over 3000 species from the  $\beta$ -stability line to the neutron drip line including light neutron-rich unstable nuclei (Terasawa et al. 2001), which are connected by more than 10,000 nuclear reactions and the neutrino-processes. In this paper we use one trajectory corresponding to the same mass region in each model calculation and adopted the time evolutions of  $T$  and  $\rho$  in order to calculate the r-process abundances. Note that we can get nearly the same abundance pattern for all trajectories except for the edge of calculated region. We start the network calculations of the nucleosynthesis at the time when the temperature drops to  $T_9 = 9.0$ , which refers to the time  $t = 0.0$  s, and follow the time evolution of the abundances.

We show in Fig. 2 the calculated final abundance patterns as a function of mass number. The dashed, solid, and dotted lines are the results in the cases of  $P_{out} = 10^{20}$ ,  $10^{21}$ , and  $10^{22}$  dyn/cm<sup>2</sup>, respectively, as in Fig. 1. For comparison the solar system r-process abundance pattern (Käppeler et al. 1989) is shown by points in arbitrary unit. When we adopt the outer boundary pressure of  $P_{out} = 10^{20}$  dyn/cm<sup>2</sup>, the characteristic three peaks in the r-process abundance pattern are well reproduced at around  $A \sim 80, 130$  and  $195$ . On the other hand, in the case of  $P_{out} = 10^{21}$  dyn/cm<sup>2</sup>, 3-rd peak elements are underabundant. In the highest pressure model with  $P_{out} = 10^{22}$  dyn/cm<sup>2</sup>, the nuclear reaction flow stops at the region of only the 2-nd peak, and the 3-rd peak elements are not formed at all. From this figure we can see that more abundant heavy elements are synthesized as  $P_{out}$  is lower. Since there is a clear and reasonable relation between  $T_{out}$  and  $P_{out}$  (Table 1 and Fig. 1), we can conclude that heavier r-process elements are more abundantly synthesized when  $T_{out}$  is lower. We will describe the reasons for this later.

Let us discuss the mechanism of the nucleosynthesis quantitatively more in detail. The r-process nuclei are synthesized by two sequential processes, alpha-process and r-process (Woosley and Hoffman 1992). Near the surface of neutron star the matter maintains the nuclear statistical equilibrium (NSE) and there are only free neutrons and protons because of the high temperature ( $T_9 \sim 30$ ). When the temperature becomes lower than  $T_9 \sim 10$ , free neutrons and protons begin to assemble into composite nuclei.

In Fig. 1, the abundance of alpha particles,  $Y_\alpha$ , in the upper panel, and the abundance of seed nuclei,  $Y_{seed}$ , and the neutron-to-seed ratio,  $Y_n/Y_{seed}$ , in the lower panel are shown as a function of time when the temperature becomes  $T_9 < 9$ . The value of  $Y_\alpha$ , at first, rapidly increases in the NSE. As the temperature decreases, the system is gradually out of NSE, and  $Y_{seed}$  starts increasing when  $Y_\alpha$  approaches the peak abundance around  $T_9 \sim 5$ . After this time, alpha particles are gradually consumed by the alpha-process in order to produce neutron-rich seed nuclei with mass number  $A \sim 100$ . The peak position of  $Y_\alpha$  is different in the three models for different outer boundary pressures because of the difference in the dynamical timescale. Note, however, that this difference in the timescale makes a smaller influence on the nucleosynthesis than the influence arising from different  $T_{out}$ . As the temperature becomes lower, charged particle reactions become rapidly slower, and alpha-captures also cease when the temperature becomes close to  $T_9 < 2$  towards the alpha-rich freezeout. At this time and temperature the composition changes to neutrons, alphas, and a little amount of seed nuclei. The r-process starts from these seed nuclei and makes heavy r-process elements. Heavy elements are synthesized more abundantly, as the number of neutrons per seed nucleus,  $Y_n/Y_{seed}$ , becomes larger. Finally, neutrons are almost consumed and  $Y_{seed}$  eventually reaches almost constant value. At this freezeout time of the r-process, the nuclear flow almost ceases and produced neutron-rich nuclei begin to convert into stable nuclei, smoothing the abundance pattern by  $\beta$ -decays and  $\beta$ -delayed neutron emissions.

The  $Y_n$  values are almost the same in our three models because entropies are almost the same (Table 1). The important factor to make the difference in final abundance pattern is the abundance of seed nuclei. In the model with a short dynamical timescale for  $P_{out} = 10^{20}$  dyn/cm<sup>2</sup> and  $T_{out} \sim 0.4$ , since the temperature drops rapidly (see the dashed line in upper panel of Fig. 1), the alpha-process does not proceed efficiently as it does in the slow expansion model like Woosley’s flow (Woosley et al. 1994). This is because charged particle reactions occur at high temperatures. There are relatively small amount of seed nuclei produced near the boundary region where the temperature drops to  $T_{out}$ . This scenario, however, tacitly assumes that the temperature is so low as not to operate the alpha-process efficiently. If, on the other hand, the temperature is high ( $T_{out} \geq 1.0$ ) in the outer boundary region, alpha captures can frequently occur to the same or even greater extent as neutron captures. The seed nuclei continue to be made by the alpha-process in such cases.

This mechanism makes the biggest influence on the seed abundance and the r-process nucleosynthesis as well. When  $T_{out}$  is high,  $Y_{\alpha,out}$  is small and  $Y_{seed,out}$  is large (Table 1 and Fig. 1). As a result, in the high pressure model,  $Y_n/Y_{seed}$  is smaller than the other low pressure models, and the heavy elements cannot be synthesized, as shown in Fig. 2. In the case of the low pressure model, on the contrary, the temperature is as low as  $T_9 \sim 0.4$  in the outer boundary region. Therefore, even after the alpha-rich freezeout there are plenty of free

neutrons with relatively smaller amount of seed elements, because the alpha captures are suppressed due to the low temperature, and the r-process proceeds creating heavy elements at the 3rd r-process peak abundantly (the dashed curve in Fig. 2).

#### 4. Discussions and Conclusion

We showed a possibility that the r-process can successfully occur in the neutrino-driven winds from a neutron star having typical observed neutron star mass,  $1.4M_{\odot}$ , provided that the outer boundary condition is appropriately chosen. More specifically from Fig. 1, we can conclude that the model with  $P_{out} = 10^{20}$  dyn/cm<sup>2</sup> (dashed line) is most likely in the neutron star model with  $M_{NS} = 1.4M_{\odot}$  and  $R_{NS} = 10$  km. In the present model the dynamical timescale is a few times longer than the previous successful models and the entropy per baryon is relatively low,  $100 - 200$  k<sub>B</sub>.

This conclusion results from the fact that the alpha captures do not efficiently work as the outer boundary temperature,  $T_{out}$ , becomes lower. We can reconfirm this effect quantitatively in the following way. If the seed nuclei are synthesized only by the alpha-process and the seeds do not change to other heavy nuclei approximately, the decrease in alpha particles from the peak value in Fig. 1 is equal to the increase in the seeds. Then, the relation,  $\Delta Y_{\alpha} \times 4 = \Delta Y_{seed} \times 100$ , follows due to the mass conservation, where we assume the averaged mass number of seed nuclei 100. We could confirm actually that this relation holds very well in final abundances ( $Y_{seed,out}$  and  $Y_{\alpha,out}$ ) in our three models (Table 1).

It is generally believed that the neutron star mass depends somewhat on the progenitor mass (Woosley & Weaver 1995, Thielemann et al. 1996, Timmes et al. 1996, Limongi et al. 2000). The physical conditions that govern the r-process are determined by  $S$ ,  $Y_e$ , and  $\tau_{dyn}$ , which also strongly depend on the neutron star mass. However, recent observations of neutron-capture elements in metal-deficient stars show the universality in the abundance pattern for the r-process elements with  $56 \leq Z \leq 70$  (Snedden et al. 2000, Westin et al. 2000, Cayrel et al. 2001, Honda 2002). They suggest that the universal r-process abundance pattern should be realized independent of the neutron star mass. Let us consider the dependence of abundance pattern on the neutron star mass by using the same outer boundary pressures. We adopt several neutron star mass of 1.2, 1.3, 1.4, 1.5 and  $1.6M_{\odot}$  in the simulations of the neutrino-driven winds (Terasawa 2002 and Terasawa et al. 2002). These masses cover the almost all observed neutron star masses except for a few neutron stars (Bulik et al. 1995, Brown et al. 1996, Thorsett and Chakrabarty 1999, Barziv et al. 2001, and references therein).



As for the outer boundary conditions, we varied the pressure values as  $P_{out} = 10^{20}, 10^{21}$ , and  $10^{22}$  dyn/cm<sup>2</sup> in our simulations of the  $1.2 - 1.6M_{\odot}$  models. The value of  $S$  is higher and  $\tau_{dyn}$  is shorter as the neutron star mass becomes larger, although  $Y_{e,i}$  are almost the same  $\sim 0.43 - 0.44$  in all calculations, which we have carried out, and  $T_{out}$  is common for each value of  $P_{out}$ . As discussed in the previous section, we saw that  $Y_{\alpha,out}$  becomes smaller and  $Y_{seed,out}$  becomes larger with increasing pressure for the fixed neutron star mass. On the other hand, for the fixed outer boundary pressure,  $Y_{\alpha,out}$  becomes larger and  $Y_{seed,out}$  becomes smaller as the neutron star mass becomes larger. From these systematics which we found, we understand that more abundant heavy elements are synthesized as the neutron star mass is larger and the outer boundary pressure becomes lower. In the previous study of the r-process nucleosynthesis in neutrino-driven winds (Sumiyoshi et al. 2001), the outer boundary pressure was set equal to  $P_{out} \sim 10^{22}$  dyn/cm<sup>2</sup> for both neutron star mass models of  $1.4M_{\odot}$  and  $2.0M_{\odot}$ . This pressure ( $P_{out} \sim 10^{22}$  dyn/cm<sup>2</sup>) corresponds to the temperature  $T_{out} \sim 0.1$  MeV. By their calculations, when this value was adopted in the  $1.4M_{\odot}$  model, the flow of nucleosynthesis virtually stopped at the nuclear mass region below the 2-nd peak. Therefore, a higher neutron star mass model ( $2.0M_{\odot}$ ) was adopted to increase the entropy for a successful r-process. This theoretical correlation among  $P_{out}$ ,  $T_{out}$ , and  $M_{NS}$  is reasonably understood, that is a higher outer boundary pressure corresponds to a higher neutron star mass, and vice versa. However, it is to be stressed that increasing boundary pressure and temperature leads to unsuccessful r-process without increasing the neutron star mass. In the present study we find another condition to realize successful r-process namely by adopting suitable outer boundary condition with keeping the neutron star properties as those measured observationally, i.e.  $M_{NS} \sim 1.4M_{\odot}$  and  $R_{NS} \sim 10$  km. This result makes a strong constraints on modeling the dynamics of supernova explosion in view of constructing the structure model of massive progenitor stars in order to clarify the physical conditions of the r-process nucleosynthesis.

One of the authors (MT) wishes to acknowledge the fellowship of the Japan Society for Promotion of Science (JSPS) and would like to thank Professor K. Ikeda and Dr. N. Itagaki for helpful discussions. This work is in part supported by JSPS under the Grants-in-Aid Program for Scientific Research (10640236, 10044103, 11127220, 12047230, 12047233, 13002001, 13640313, 13740165, 14039210) of for the Ministry of Education, Science, Sports, and Culture of Japan.

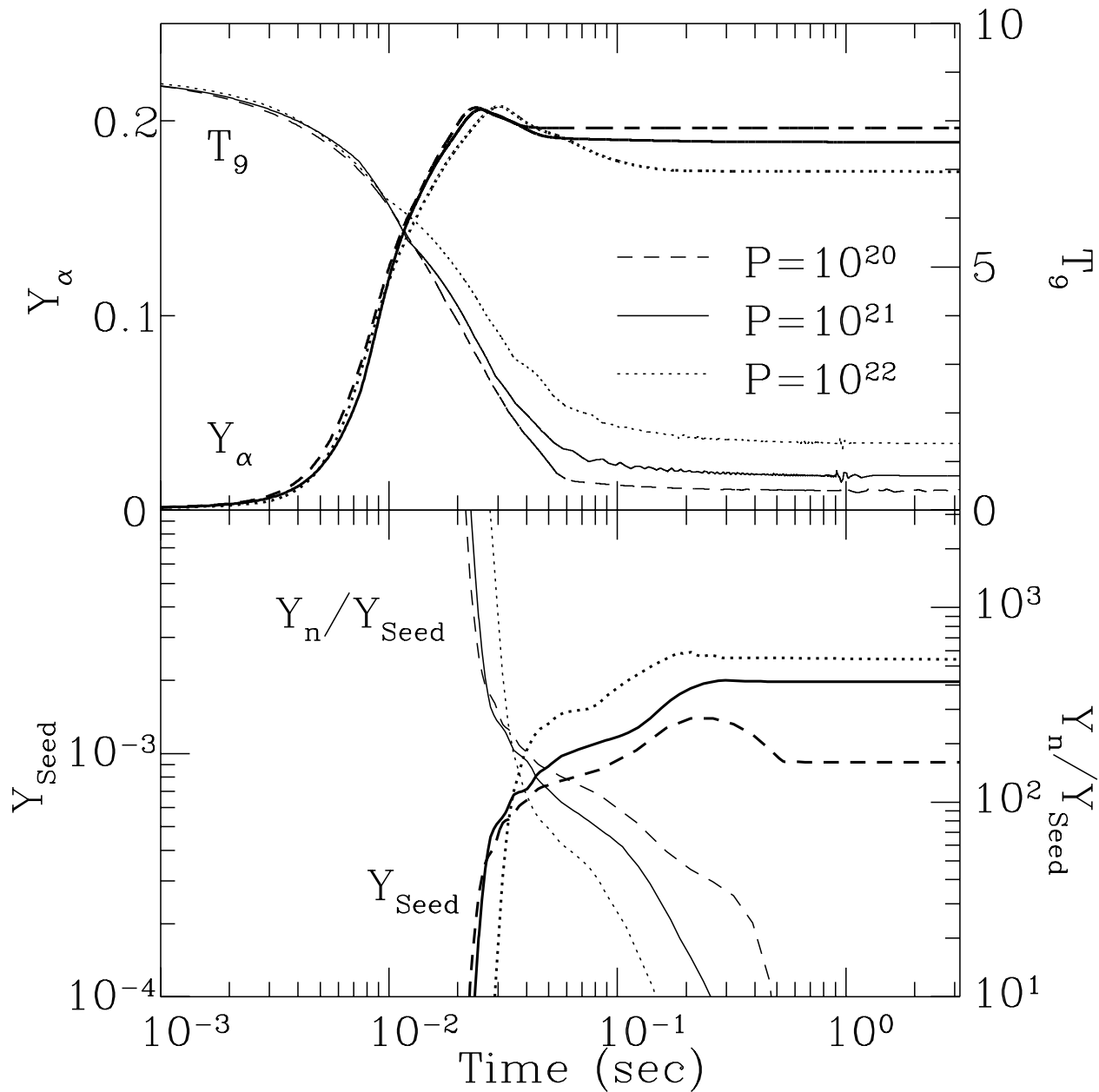


Fig. 1.— Time variations of the alpha-particle abundance,  $Y_\alpha$ , and temperature  $T_9$  (upper panel), and neutron-to-seed ratio,  $Y_n/Y_{seed}$ , and seed abundance,  $Y_{seed}$  (lower panel). The dashed, solid, dotted lines are the results in the cases of  $P_{out} = 10^{20}$ ,  $10^{21}$ , and  $10^{22}$  dyn/cm<sup>2</sup>, respectively.

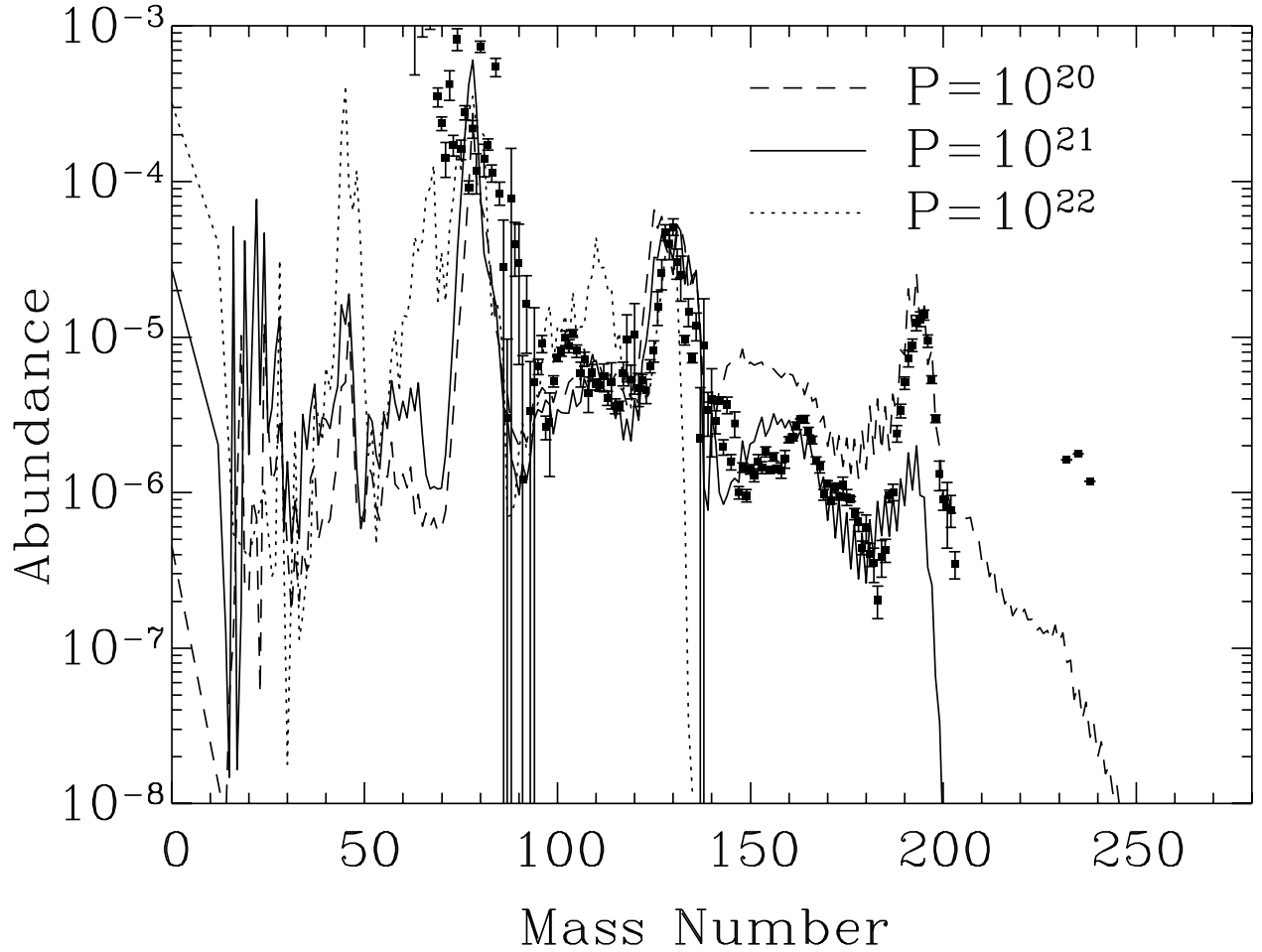


Fig. 2.— Final abundance yields as a function of the mass number. The dashed, solid, dotted lines are the same as those in Fig. 1. Data points are the solar r-process abundances in arbitrary unit from Käppeler et al. (1989).

## REFERENCES

- Barziv, O., Kaper, L., Van Kerkwijk, M. H., Telting, J. H., and Van Paradijs, J., 2001, *A & A*, 377, 925
- Brown, G. E., Weingartner, J. C., Wijers, and Ralph A. M. J., 1996, *ApJ*, 463, 297
- Bulik, T., Riffert, H., Meszaros, P., Makishima, K., Mihara, T., and Thomas, B., 1995, *ApJ*, 444, 405
- Burbidge, E. Margaret, Burbidge, G. R., Fowler, William A., Hoyle, F. 1957, *Rev. Mod. Phys.*, 29, 547.
- Cayrel, R., Hill, V., Beers, T. C., Barbuy, B., Spite, M., Spite, F., Plez, B., Andersen, J., Bonifacio, P., Francois, P., Molaro, P., Nordstrom, B., Primas, F., 2001, *Nature*, 409, 691
- Honda, S. et al. (SUBARU/HDS Collaboration), 2002, in preparation
- Johnson, J. A., Bolte, M., 2001, *Nucl. Phys*, A688, 41
- Käppeler, F., Wiescher, M., Giesen, U., Goerres, J., Baraffe, I., El Eid, M., Raiteri, C. M., Busso, M., Gallino, R., Limongi, M., and Chieffi, A., 1989, *ApJ*, 437, 396
- Limongi, M., Straniero, O., Chieffi, A., 2000, *ApJ*, 129, 625
- Meyer, B. S. 1995, *ApJ. Lett.*, 449, 55
- Otsuki, K., Tagoshi, H., Kajino, T., and Wanajo, S. 2000, *ApJ*, 533, 424
- Qian, Y. -Z. and Woosley, S. E. 1996, *ApJ*, 471, 331
- Shen, H., Toki, H., Oyamatsu, K., and Sumiyoshi, K. 1998a, *Nucl. Phys. A*, 637, 435
- Shen, H., Toki, H., Oyamatsu, K., and Sumiyoshi, K. 1998b *Prog. Theor. Phys.*, 100, 1013
- Snedden, C., Cowan, J. J., Debra, L. B., and Truran, J. W. 1998, *ApJ*, 496, 235
- Snedden, C., Cowan, J. J., Ivans, I. I. Fuller, G. M. Burles, S., Beers, T. C., and Lawler, J. E. 2000, *ApJ*, 533, L139
- Snedden, C., McWilliam, A., Preston, G. W., Cowan, J. J., Burris, D. L., and Armosky, B. J. 1996, *ApJ*, 467, 819

- Sumiyoshi, k., Suzuki, H., Otsuki, K., Terasawa, M., and Yamada, S. 2000, Pub. Astron, Soc. Japan 52, 601
- Terasawa, M., Sumiyoshi, K., Kajino, T., Tanihata, I., and Mathews, G. J. 2001, ApJ, Vol. 562, pp. 470-479
- Terasawa, M. 2002, PhD Thesis, University of Tokyo
- Terasawa, M., Sumiyoshi, K., Yamada, S., Suzuki, H. 2002, in preparation
- Thielemann, F. K., Nomoto, K., and Hashimoto, M. 1996, ApJ, 460, 408
- Timmes, F. X., Woosley, S. E., Weaver, Thomas A., 1996, ApJ, 457, 834
- Thorsett, S. E., and Chakrabarty, D., 1999, ApJ, 512,288
- Westin, J., Sneden, C., Gustafsson, B., and Cowan, J. J. 2000, ApJ, 530, 783
- Woosley, S. E. and Hoffman, R. D. 1992, ApJ, 395, 202
- Woosley, S.E. and Weaver, T.A. 1995, ApJS, 101, 181
- Woosley, S. E., Wilson, J. R., Mathews, G. J., Hoffman, R. D., and Meyer, B. S. 1994, ApJ, 433, 229
- Yamada, S. 1997, ApJ, 475, 720
- Yamada, S. Janka, H.-Th., and Suzuki, H. 1999, A&A, 344, 533

Table 1. The Key Quantities for the r-Process Nucleosynthesis.

$P_{out}$ [dyn/cm <sup>2</sup> ]	$\tau_{dyn}$ [sec]	$S$ [ $k_B$ ]	$Y_{e,i}$	$T_{out}$ [ $10^9$ K]	$Y_{\alpha,out}$	$Y_{seed,out}$
$10^{20}$	$2.32 \times 10^{-2}$	200	0.43	0.4	0.196	$9.2 \times 10^{-4}$
$10^{21}$	$2.54 \times 10^{-2}$	180	0.43	0.7	0.189	$2.0 \times 10^{-3}$
$10^{22}$	$3.34 \times 10^{-2}$	170	0.44	1.3	0.174	$2.4 \times 10^{-3}$

Note. — The summary of model parameters and key quantities for the r-process.  $P_{out}$  is the pressure at the outer boundary and we give these values as an outer boundary condition.  $\tau_{dyn}$ ,  $S$ , and  $Y_{e,i}$  are the dynamical timescale, entropy per baryon, and initial electron fraction, respectively. Note that the definition of  $\tau_{dyn}$  is the  $e$ -fold time at  $T = 0.5$  MeV.  $Y_{\alpha,out}$  and  $Y_{seed,out}$  are the final abundances of alpha-particles and seed nuclei.